

# Polyvinylidene fluoride-based Nanocomposite Films Induced by Exfoliated Boron Nitride Nanosheets with Controlled Orientation

Hong-Baek Cho<sup>\*,\*\*</sup>, Tadachika Nakayama<sup>\*\*†</sup>, DaeYong Jeong<sup>\*\*\*</sup>, Satoshi Tanaka<sup>\*\*</sup>,  
Hisayuki Suematsu<sup>\*\*</sup>, Koichi Niihara<sup>\*\*</sup>, Yong-Ho Choa<sup>\*†</sup>

**ABSTRACT:** Polyvinylidene fluoride (PVDF)-based nanocomposites are fabricated by incorporation of boron nitride (BN) nanosheets with anisotropic orientation for a potential high thermal conducting ferroelectric materials. The PVDF is dissolved in dimethylformamide (DMF) and homogeneously mixed with exfoliated BN nanosheets, which is then cast into a polyimide film under application of high magnetic fields (0.45~10 T), where the direction of the filler alignment was controlled. The BN nanosheets are exfoliated by a mixed way of solvothermal method and ultrasonication prior to incorporation into the PVDF-based polymer suspension. X-ray diffraction, scanning electron microscope and thermal diffusivity are measured for the characterization of the polymer nanocomposites. Analysis shows that BN nanosheets are exfoliated into the fewer layers, whose basal planes are oriented either perpendicular or parallel to the composite surfaces without necessitating the surface modification induced by high magnetic fields. Moreover, the nanocomposites show a dramatic thermal diffusivity enhancement of 1056% by BN nanosheets with perpendicular orientation in comparison with the pristine PVDF at 10 vol % of BN, which relies on the degree of filler orientation. The mechanism for the magnetic field-induced orientation of BN and enhancement of thermal property of PVDF-based composites by the BN assembly are elucidated.

**Key Words:** Polyvinylidene fluoride, Boron nitride nanosheets, Anisotropic orientation, Thermal diffusivity

## 1. INTRODUCTION

Ferroelectric polymer composites with high dielectric constants and high thermal conductivity plays a critical role in modern electronics and electric industry, and particularly, for electric energy storage (EES) of electric power system and thermal management application [1-3]. EES is the capability of storing energy or electricity in order to produce electricity and releasing it, which is also very promising for modern electronics and electric power systems [4]. Among the recent EES devices, such as fuel cells, batteries, capacitors, and supercapacitors, capacitors possess the advantage of high power density due to their fast electrical energy charge-discharge

capability [5,6]. Comparing to recently introduced polymer capacitors ( $\sim 3 \text{ Jcm}^{-3}$ ) [7,8], the energy densities of commercial capacitors such as batteries and electric capacitors are still high around 10 times [9], while polymer capacitors are potential in view of the extended life span, easier processing, operation under the higher voltages, reduction of the volume, light in weights and lower cost of the electric power systems for advanced electric [10-12].

The total energy density of capacitors of linear dielectric,  $U$ , is calculated by:

$$U = \int \frac{1}{2} K \epsilon_0 E^2 \quad (1)$$

Received 24 September 2015, received in revised form 26 October 2015, accepted 27 October 2015

<sup>\*†</sup>Department of Materials Science & Chemical Engineering, Hanyang University, Ansan 426-791, Korea  
Corresponding author (E-mail: [choa15@hanyang.ac.kr](mailto:choa15@hanyang.ac.kr))

<sup>\*\*†</sup>Extreme Energy-Density Research Institute, Nagaoka University of Technology, Nagaoka 940-2188, Japan  
Corresponding author (E-mail: [nky15@vos.nagaokaut.ac.jp](mailto:nky15@vos.nagaokaut.ac.jp))

<sup>\*\*\*</sup>Department of Materials Science & Engineering, Inha University, Incheon 402-751, Korea

These authors contributed equally to this work.

where  $E$  is the applied electric field,  $K$  is the dielectric constant and  $\epsilon_0$  is the vacuum permittivity [8,13]. Therefore,  $U$  relies on both  $K$  and  $E$ , where  $E$  is limited by high electric breakdown field ( $\epsilon_{bd}$ ). However, the dielectric polymer films utilized in energy storage capacitors such as polypropylene, polyester, polycarbonate and PVDF have low dielectric constant,  $K$  ( $<3$ ) which practically limits the total energy density of capacitors ( $U$ ) [14-17]. In order to overcome the limitation of the  $K$ , various ferroelectric oxides such as  $\text{BaTiO}_3$ ,  $(\text{Pb}, \text{La}) \text{TiO}_3$  with high dielectric constant ranging from hundreds to thousands have been incorporated into the polymers [18-20] obtaining the sharp increase of  $K$ , whereas suffer from significantly decreased  $\epsilon_{bd}$  which results in restricting the application in higher power system as capacitors. Efforts have been focused on resolving the issue of fabricating polymer nanocomposites with high  $K$  while maintaining the high  $\epsilon_{bd}$  in dielectric capacitors. The covalent incorporation of tantalum species into ferroelectric polymers via in-situ sol-gel condensation, incorporation of low dielectric boron nitride (BN) in PVDF [21],  $\text{SiO}_2$  coated reduced graphene oxide nanosheets in PVDF [22] have showed elevated  $\epsilon_{bd}$  of composites with  $K$  less than or no higher than the pristine polymer matrix. Application of hexagonal BN (h-BN) of graphite-like layered structure is reported to be efficient for the decrease of  $\epsilon_{bd}$  of composites owing to its wide band gap (5.5~6.4 eV) insulating property with a dielectric strength ( $\sim 800 \text{ MV m}^{-1}$ ) [23].

In view of high thermal conducting property of dielectric materials, the thermal management emerges as one of big issue as the needs for cooling the electronic devices for higher power systems are constantly increasing according to miniaturization of devices [3]. Most of dielectric polymers that can offer excellent dielectric property and superior processibility have low thermal conductivity ( $<0.3 \text{ W/m}\cdot\text{K}$ ) [24,25], which cannot satisfy the currently required range of thermal conductivity in industry 1~5  $\text{W/m}\cdot\text{K}$  [26] without incorporation of fillers with high thermal conductivity.

In this work, we demonstrate a new design of ferroelectric polymer nanocomposites as potential high thermal conductive polymer capacitors through controlled orientation of insulating BN ceramics without giving variation of the filler contents. Here, we apply hexagonal BN as a filler for controlling thermal conducting route by modulating their orientation because h-BN has intrinsic thermal anisotropy depending on its orientation; in-plane thermal conductivity of h-BN (600  $\text{W/m}\cdot\text{K}$ ) is 20 times higher than out-of-plane thermal conductivity (3  $\text{W/m}\cdot\text{K}$ ) [27]. We carry out the exfoliation of layered hexagonal BN, incorporation of the exfoliated BN with anisotropic orientation under application of magnetic fields, evaluation of thermal property of composites and elucidation over mechanism of filler-orientation under given magnetic fields and enhancement of thermal diffusivity as a function of anisotropic orientation of BN nanosheets.

## 2. EXPERIMENTAL

### 2.1 Materials

As-received hexagonal boron nitride nanosheets (BN nanosheets) ( $D_{90} = 17.1 \mu\text{m}$ , aspect ratio = 228.0) of commercial origin (Denka) is used as a dielectric filler. The morphological characteristics of these nanosheets are described elsewhere [28]. A PVDF (molecular weight<sub>av</sub> =  $\sim 534,000$ ) from Sigma-Aldrich Co. is used as a polymer matrix. N, N-dimethylformamide (DMF) from Kanto Chemical Co. INC. is used as a polar solvent.

### 2.2 Exfoliation of BN nanosheets

Exfoliation of BN nanosheets by solvothermal method is carried out by a modified way of solvothermal method [29] followed by ultra-sonication for the enhancement of physical detachment of layer-by-layer BN nanosheets. For exfoliation of BN nanosheets by solvothermal method, 4 g of h-BN powder is introduced into a solvent mixture of solvent  $\text{H}_2\text{O}/\text{DMF}$  (1:20 vol%) and reacted in an autoclave at  $180^\circ\text{C}$  for 24 h. The product is underwent the physical exfoliation by sonication-assisted method by tip-type sonication (500 W, duty cycle 30%, output control 2) for 10 h at  $10^\circ\text{C}$ . The resulting suspension is centrifuged under 3000 rpm for 40 minutes and the supernatant is recovered for the next step, which is further centrifuged under 1000 rpm for precipitation of exfoliated BN nanosheets and recovered followed by drying for overnight at  $120^\circ\text{C}$ .

### 2.3 Application of high magnetic fields

PVDF/BN nanosheets composites with controlled orientation of BN nanosheets were prepared by the following method. 900 mg of PVDF powder is dissolved in 43 mL of DMF by tip-type sonication for 30 minutes. 100 mg of the exfoliated BN nanosheets is added to the suspension and sonicated for 30 minutes. The suspension was then cast on a glass spacer (12 mm  $\times$  12 mm  $\times$  100  $\mu\text{m}$ ), staged inside of a cylinder-like magnet and subjected to a 0.45 and 10 T (see Fig. 1) magnetic fields, superconducting type, for 8 h under  $80^\circ\text{C}$  to enhance either the perpendicular or parallel alignment of the BN nanosheets in the suspension of PVDF and DMF solution. During application of a magnetic field (10 T), the stage of samples are rotated with 60 revolutions per minute (rpm) (a rotation magnet) or fixed as static status (a static magnet) for the comparison of rotation effects. Finally, the prepared composite films were withdrawn from the magnetic field, peeled from supporting glass plate and further dried for 24 h at  $120^\circ\text{C}$  under vacuum for the complete removal of residual solvent. The exfoliated BN nanosheets and resulting composites are characterized by scanning electron microscopy (SEM), transmission electron microscopy (TEM) and X-ray diffraction (XRD). The thermal properties of the prepared composites

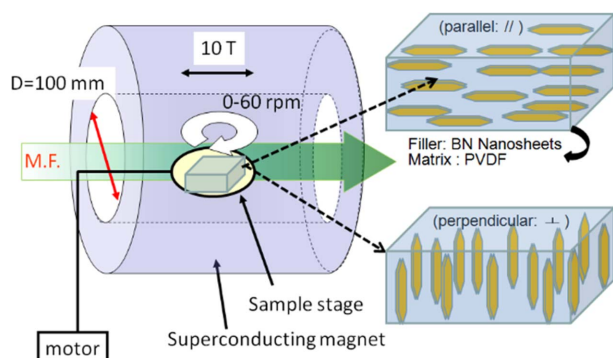


**Fig. 1.** Experimental set-up for controlled orientation of BN nanosheets in PVDF under magnetic field (\*M.F.: magnetic force)

were analyzed using a system for measuring the thermal diffusivity that is based on temperature wave analysis (ai-Phase Mobile 1, ai-Phase Co.). Each composite film was measured five times, which guarantees  $\pm 3\%$  of standard deviation.

### 3. RESULTS AND DISCUSSION

#### 3.1 Magnetic field-induced orientation of BN nanosheets

Fig. 2 shows SEM micrographs of BN nanosheets before and after exfoliation. Through solvothermal reaction and ultrasonication, layered structures of BN nanosheets (Fig. 2-a) are exfoliated and the surface morphology are varied as shown in Figs. 2-b,-c and -d. There still remain BN nanosheets which are not completely exfoliated, but shows exfoliated BN nanosheets in many domains existing as rolled, folded and bent status, where some others are located as debris on the surface of the BN planes. For an effective exfoliation of h-BN by chemical way, use of strong solvents was considered to be appropriate [30] because a strong interaction occurs between

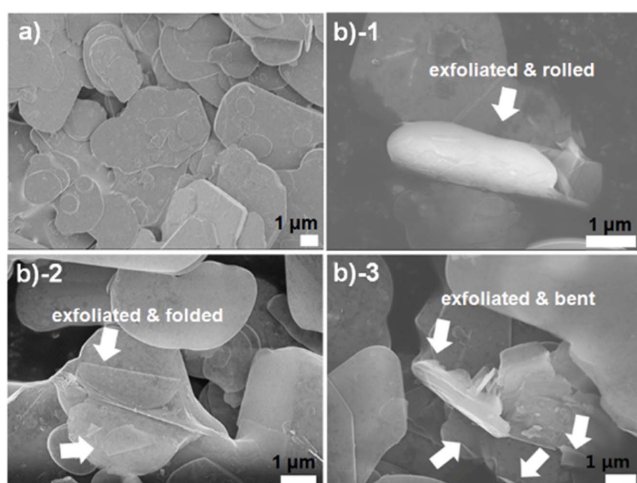


**Fig. 2.** SEM images of BN nanosheets a) before and b) after exfoliation resulting from solvothermal reaction and ultra-sonication

the polar molecules of solvent and a h-BN surface, which facilitates overcoming the van der Waals force between lay-by-layer of BN while peeling the BN nanosheets.

The application of ultrasolication for exfoliation of BN was intended for facilitation of separation of exfoliated BN nanosheets [31], which was influential to obtain the fewer-layer h-BN. While the few-layered h-BN obtained in aqueous dispersion by sonication-assisted hydrolysis promoted the cutting of the h-BN resulting in the reduced lateral dimension as observed debris on BN surface (see Fig. 2b).

The X-ray diffraction pattern of BN in Fig. 3 shows the degree of anisotropic orientation of BN perpendicular to the film surfaces. The thickness of the spacer during magnetic field-induced preparation was 100  $\mu\text{m}$  (see Experimental), and the average thickness of the finally obtained composites could be controlled to  $_{av}15 \mu\text{m}$  depending on the volume ratio of BN nanosheets to the solvent mixture. Under application of magnetic field of 10 T, (002) plane of BN ( $2\theta = 26.76^\circ$ ) with random distribution starts to decrease from  $2.69 \times 10^5$  to  $2.26 \times 10^5$  by static magnet, which was further decreases to  $2.25 \times 10^5$  by rotation magnet. This denotes that the population of BN nanosheets with parallel arrangement in the composite film surface decreased influenced by the application of magnetic fields. It is noticeable that the average length of BN is longer than the film thickness,  $_{av}15 \mu\text{m}$ , and no variation of (100) plane intensity (at  $2\theta = 41.60^\circ$ ), which is typically shown in the other researches with incorporation of BN with vertical orientation [32], is observed. This phenomenon can be explained from that the lateral dimension of BN nanosheets, 17.1  $\mu\text{m}$ , is longer than the final thickness of composites, which renders the cross-sectional status of the oriented BN nanosheets slant-like structure as illustrated in Fig. 3. Furthermore, it is meaningful that the orientation of BN nanosheets are controlled without modifying the surface with magnetite such as  $\gamma$ -iron oxide [33].

The morphology of composite surfaces with perpendicular

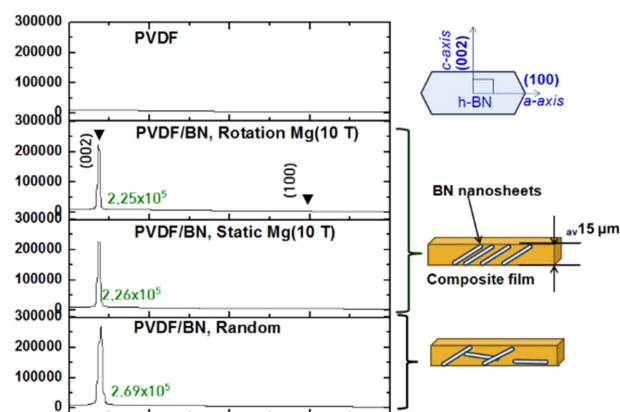


**Fig. 3.** X-ray diffraction pattern of composites according to BN nanosheets with different degree of perpendicular orientation

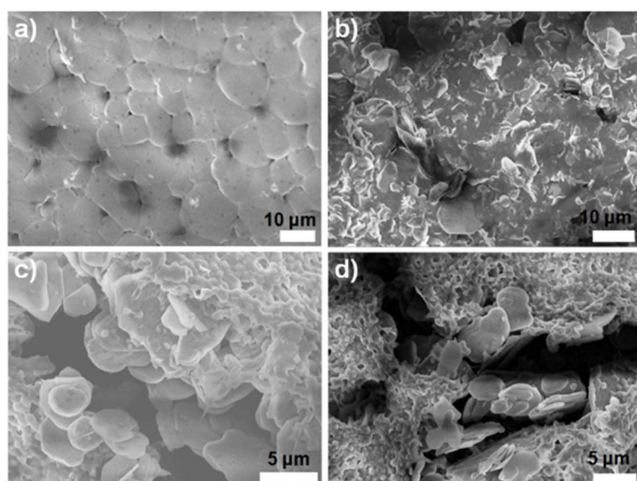


**Fig. 4.** Surface SEM images of composites with embedded BN nanosheets in composite films before (a) and after exfoliation (b~d); a) PVDF/BN, Random, b) PVDF/BN, Random, c) PVDF/BN ( $\perp$ ), Static Mg (10T), and d) PVDF/BN ( $\perp$ ), Rotation Mg(10T). (\* Rt Mg: rotation magnet, St. Mg: static magnet, BN content: 10 vol %)

orientation of BN nanosheets are shown in Fig. 4. The composite surfaces with random distribution of BN show very different morphology before (Fig. 4-a) and after (Fig. 4-b) exfoliation of the BN nanosheets. Among composites with incorporation of randomly distributed BN nanosheets (Figs. 4-a & -b), a composite embedded with pristine BN shows relatively smooth surface rather than with exfoliated BN that shows rough surface due to the uneven surface induced-by exfoliation and the fewer layered-BNs.

Under application of strong magnetic field, the surface of the composites has many cracks which became severer as the source of magnetic flux was changed from static magnet to rotation magnet. The slant-like BN planes (Figs. 4-c & -d) of BN planes, viewed through the cracks of magnified SEM micrographs shows that the BN nanosheets are not completely oriented perpendicular to the composite surfaces, which is coincidence to the upper description over XRD patterns in Fig. 3.

It was considered that the film surfaces were automatically severed by the BN nanosheets with perpendicular orientation as the DMF solvents occupying 90 vol % of the polymer suspension was disappeared by evaporation at temperature of 80°C and then at temperature of 120°C (see Experimental).

### 3.2 Physical properties

Thermal diffusivity is an important parameters for estimating the thermal conductivity of polymer-based composite materials [34]. When randomly distributed BN nanosheets are compared, a composite with exfoliated BN enhanced the thermal diffusivity to 141% comparing to the one with untreated BN. The thermal property increased as the degree of per-

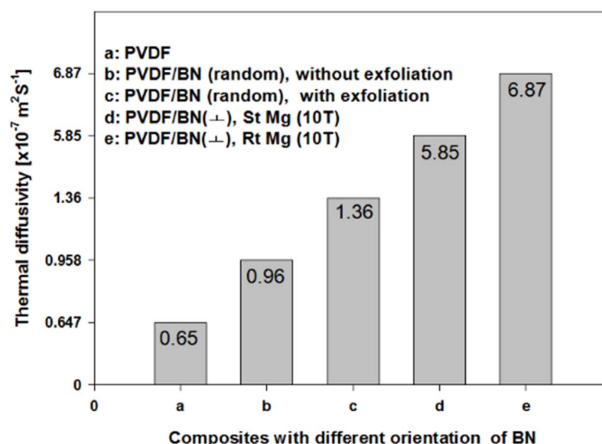


**Fig. 5.** Variation of thermal diffusivity of composites under application of magnetic fields (perpendicular orientation) (BN contents: 10 vol %)

pendicular orientation is enhanced by application of static magnet and then by rotation magnet. Finally the composite prepared under application of rotation magnet showed thermal diffusivity to  $6.87 \times 10^{-7} \text{ m}^2 \text{ s}^{-1}$ , which is increase of 715% rather than composite with incorporation of untreated BN of the same content and 1056% in comparison with the neat PVDF. Estimating from the surface morphology of the composites, the composite prepared under application of rotation magnet, Fig. 4-d, shows the highest domains of cracks on the surface which is considered to hinder the thermal conduction. Instead, the BN nanosheets with perpendicular orientation are connecting from one side of the film to the opposite side. This direct route of high thermal conductivity is regarded to increase the resulting composite over 7 times rather than the corresponding one with smooth surfaces (Fig. 4-a). It is more understandable if the thermal conductivity of in-plane direction h-BN is 600 W/m·K [35] which is 700% higher than that of PVDF (<0.3 W/m·K) [24,25] implying that the importance of building high thermal conducting routes with high thermal-conducting filler.

The surfaces of composite films with random distribution of exfoliated BN nanosheets showed rough surface morphology without cracks. And the magnetic field-induced orientation of BN nanosheets implied that the direction of BN planes could be well-controlled without necessitating the surface modification, which attributed to the enhancement of thermal property of the resulting composites. This technique is potential for the development of high thermal conducting polymer materials in power electronic devices. Further researches should be done for reducing domains of cracks generated through the composite induced-by the exfoliated BN planes.

### 3.3 Discussion

The orientation of BN nanosheets without modification of the surface by nanoparticles having paramagnetic property is

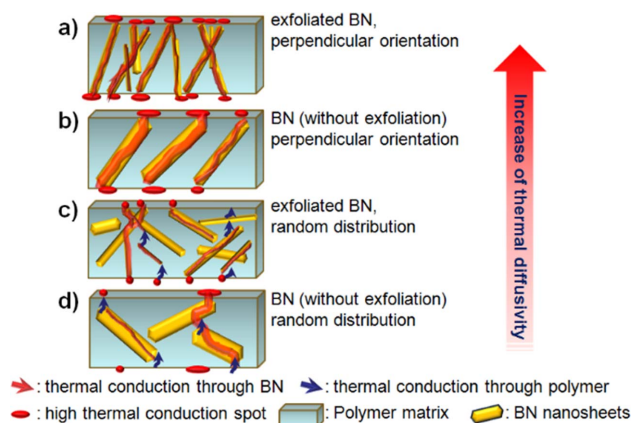


**Fig. 6.** Mechanism over generation of high thermal conducting routes by degree of perpendicular orientation of BN planes

meaningful, since the surface of graphite nanosheets are typically modified by  $\gamma\text{-Fe}_2\text{O}_3$  for the facilitation of its orientation [36]. This phenomenon can be explained by the diamagnetic field that  $c$ -axis of hexagonal-BN possess,  $-0.48 \times 10^{-6} \text{ Am}^2/\text{kg}$  [13]. It is far lower than that of paramagnetic  $\text{Fe}_2\text{O}_3$ ,  $58.6 \times 10^{-5} \text{ Am}^2/\text{kg}$  [29] and couldn't activate the orientation of BN planes under magnetic field such as 100 Oe [36], while the magnetic field higher than 0.45 T was strong enough to activate the diamagnetic susceptibility of BN in PVDF matrix for orientation control without necessitating the modification.

The thermal diffusivity of composites are enhanced as a function of degree of perpendicular orientation of BN nanosheets, whose enhancement using exfoliate BN were superior to corresponding composites without exfoliation of BN. It is explainable that the highest thermal diffusivity by Fig. 6-a) is induced by the highest population of built-in thermal conduction routes through in-plane of BN planes. It may wonder why the thermal diffusivity of Fig. 6-b) is higher than Fig. 6-c), even though the number of thermal conduction spots is larger in the case of Fig. 6-c). In order to explain this, at least four factors are related. In spite of the larger generation of thermal conduction spots, the Fig. 6-b) has the longer thermal conducting routes owing to the randomly connected BN, the thermal conduction is frequently occurred through out-of-plane direction of BN (3 W/m-K) [35] as well as in-plane direction (600 W/m-K), thickness of thermal conduction is narrower because of thinner BN nanosheets from exfoliation, possibility of thermal conduction through the routes of polymer matrix is higher rather than Fig. 6b). It is difficult to say which factor is crucial, but the coordination of these four factors seems not enough to exceed the enhancement of thermal diffusivity by straightforward connection of composite surfaces by unexfoliated BN nanosheets.

#### 4. CONCLUSIONS

PVDF-based ferroelectric polymer nanocomposites were

fabricated and their thermal and electrical properties were evaluated as a function of anisotropic orientation of insulating BN nanosheets.

We demonstrated that layered structure of BN nanosheets are exfoliated into thinner structure by mixed way of solvothermal reaction and ultra-sonication. The anisotropic orientation of BN fillers were controlled in PVDF-based nanocomposites with variation of the film thickness under application of strong magnetic field. Diamagnetic susceptibility of  $c$ -axis of BN attributed to the magnetic field-induced orientation BN, whose direction could be activated by magnetic flux higher than 0.45 T. Rotation of sample stage contributed to intensify the effect of magnetic field-inducement rather than a static magnetic field necessitating neither application of the higher magnetic field nor modification of BN surface. The composites with high anisotropic orientation of BN planes perpendicular to the composite plane increased thermal diffusivity higher than 7 times comparing with composites (10 vol% BN) with random distribution of BN and 10 times comparing with the pristine polymer.

This work for the increase of thermal property of the present nanocomposites as potential dielectric material may pave a way for comprehensive applications in power electronic and thermal management for energy systems, such as polymer capacitors and light emitting diodes.

#### ACKNOWLEDGEMENT

This research was supported by Basic Science Research Program through the National Research Foundation of Korea (NRF) funded by the Ministry of Science, ICT & Future Planning (No. 2015R1A5A1037548).

#### REFERENCES

1. Losego, M.D., Grady, M.E., Sottos, N.R., Cahill, D.G., and Braun, P.V., "Effects of Chemical Bonding on Heat Transport Across Interfaces," *Nat. Mater.*, Vol. 11, No. 6, 2012, pp. 502-506.
2. Luo, T. and Lloyd, J.R., "Enhancement of Thermal Energy Transport Across Graphene/Graphite and Polymer Interfaces: A Molecular Dynamics Study," *Adv. Func. Mater.*, Vol. 22, No. 12, 2012, pp. 2495-2502.
3. Huang, X. and Jiang, P., "Core-Shell Structured High-k Polymer Nanocomposites for Energy Storage and Dielectric Applications," *Adv. Mater.*, Vol. 27, No. 3, 2015, pp. 546-554.
4. Li, J., Claude, J., Norena-Franco, L.E., Seok, S.I., and Wang, Q., "Electrical Energy Storage in Ferroelectric Polymer Nanocomposites Containing Surface-Functionalized  $\text{BaTiO}_3$  Nanoparticles," *Chem. Mater.*, Vol. 20, No. 20, 2008, pp. 6304-6306.
5. Pikul, J.H., Gang Zhang, H., Cho, J., Braun, P.V., and King, W.P., "High-power Lithium Ion Microbatteries from Interdigitated Three-dimensional Bicontinuous Nanoporous Electrodes," *Nat. Commun.*, Vol. 4, 2013, pp. 1732.

6. Yang, Z., Zhang, J., Kintner-Meyer, M.C.W., Lu, X., Choi, D., Lemmon, J.P., and Liu, J., "Electrochemical Energy Storage for Green Grid," *Chem. Rev.*, Vol. 111, No. 5, 2011, pp. 3577-3613.
7. Rabuffi, M. and Picci, G., "Status quo and Future Prospects for Metallized Polypropylene Energy Storage Capacitors," *IEEE T. Plasma Sci.*, Vol. 30, No. 5, 2002, pp. 1939-1942.
8. Li, Q., Han, K., Gadinski, M.R., Zhang, G., and Wang, Q., "High Energy and Power Density Capacitors from Solution-Processed Ternary Ferroelectric Polymer Nanocomposites," *Adv. Mater.*, Vol. 26, No. 36, 2014, pp. 6244-6249.
9. Jiang, J., Li, Y., Liu, J., Huang, X., Yuan, C., and Lou, X.W., "Recent Advances in Metal Oxide-based Electrode Architecture Design for Electrochemical Energy Storage," *Adv. Mater.*, Vol. 24, No. 38, 2012, pp. 5166-5180.
10. Huang, C.W., Wu, C.A., Hou, S.S., Kuo, P.L., Hsieh, C.T., and Teng, H., "Gel Electrolyte Derived from Poly(ethylene glycol) Blending Poly(acrylonitrile) Applicable to Roll-to-roll Assembly of Electric Double Layer Capacitors," *Adv. Funct. Mater.*, Vol. 22, No. 22, 2012, pp. 4677-4685.
11. Song, H.K. and Palmore, G.T.R., "Redox-active Polypyrrole: Toward Polymer-based Batteries," *Adv. Mater.*, Vol. 18, No. 13, 2006, pp. 1764-1768.
12. Wang, K., Zhao, P., Zhou, X., Wu, H., and Wei, Z., "Flexible Supercapacitors Based on Cloth-supported Electrodes of Conducting Polymer Nanowire Array/SWCNT Composites," *J. Mater. Chem.*, Vol. 21, No. 41, 2011, pp. 16373-16378.
13. Lee, H., Kim, J.R., Lanagan, M.J., Trolier-Mckinstry, S., and Randall, C.A., "High-Energy Density Dielectrics and Capacitors for Elevated Temperatures:  $\text{Ca}(\text{Zr,Ti})\text{O}_3$ ," *J. Am. Ceram. Soc.*, Vol. 96, No. 4, 2013, pp. 1209-1213.
14. Zhou, Z., Carr, J., Mackey, M., Yin, K., Schuele, D., Zhu, L., and Baer, E., "Interphase/interface Modification on the Dielectric Properties of Polycarbonate/poly(vinylidene fluoride-co-hexafluoropropylene) Multilayer Films for High-energy Density Capacitors," *J. Poly. Sci., Part B: Polym. Phys.*, Vol. 51, No. 12, 2013, pp. 978-991.
15. Gui, Z., Zhu, H., Gillette, E., Han, X., Rubloff, G.W., Hu, L., and Lee, S.B., "Natural Cellulose Fiber as Substrate for Supercapacitor," *ACS Nano*, Vol. 7, No. 7, 2013, pp. 6037-6046.
16. Kahouli, A., Gallot-Lavallée, O., Rain, P., Lesaint, O., Guillermin, C., and Lupin, J.M., "Dielectric Features of Two Grades of Bi-oriented Isotactic Polypropylene," *J. Appl. Polym. Sci.*, Vol. 132, No. 28, 2015.
17. Karabelli, D., Leprêtre, J.C., Dumas, L., Rouif, S., Portinha, D., Fleury, E., and Sanchez, J.Y., "Crosslinking of Poly(vinylene fluoride) Separators by Gamma-irradiation for Electrochemical High Power Charge Applications," *Electrochim. Acta*, Vol. 169, 2015, pp. 32-36.
18. Kang, B.S., Choi, S.K., and Park, C.H., "Diffuse Dielectric Anomaly in Perovskite-type Ferroelectric Oxides in the Temperature Range of 400–700°C," *J. Appl. Phys.*, Vol. 94, No. 3, 2003, pp. 1904-1911.
19. Cohen, R.E., "Origin of Ferroelectricity in Perovskite Oxides," *Nature*, Vol. 358, No. 6382, 1992, pp. 136-138.
20. Chou, C.-C., Hou, C.-S., Chang, G.-C., and Cheng, H.-F., "Pulsed Laser Deposition of Ferroelectric  $\text{Pb}_{0.6}\text{Sr}_{0.4}\text{TiO}_3$  Thin Films on Perovskite Substrates," *Appl. Surf. Sci.*, Vol. 142, No. 1–4, 1999, pp. 413-417.
21. Han, K., Li, Q., Chanthad, C., Gadinski, M.R., Zhang, G., and Wang, Q., "A Hybrid Material Approach Toward Solution-Processable Dielectrics Exhibiting Enhanced Breakdown Strength and High Energy Density," *Adv. Funct. Mater.*, Vol. 25, No. 23, 2015, pp. 3505-3513.
22. Han, K., Li, Q., Chen, Z., Gadinski, M.R., Dong, L., Xiong, C., and Wang, Q., "Suppression of Energy Dissipation and Enhancement of Breakdown Strength in Ferroelectric Polymer-graphene Percolative Composites," *J. Mater. Chem. C*, Vol. 1, No. 42, 2013, pp. 7034-7042.
23. Dean, C.R., Young, A.F., Merici, Leec, Wang, Sorgenfreis, Watanabek, Taniguchit, Kimp, Shepard, K.L., and Honej, "Boron Nitride Substrates for High-quality Graphene Electronics," *Nat. Nano*, Vol. 5, No. 10, 2010, pp. 722-726.
24. Jinhong, Y., Xingyi, H., Chao, W., and Pingkai, J., "Permittivity, Thermal Conductivity and Thermal Stability of Poly(vinylidene fluoride)/graphene Nanocomposites," *IEEE Trans. Dielectr. Electr. Insul.*, Vol. 18, No. 2, 2011, pp. 478-484.
25. Pietralla, M., "High Thermal Conductivity of Polymers: Possibility or Dream?," *J. Comput-Aided. Mater.*, Vol. 3, 1996, pp. 273-280.
26. Balandin, A.A., "Thermal Properties of Graphene and Nanostructured Carbon Materials," *Nat. Mater.*, Vol. 10, 2011, pp. 569-580.
27. Rumyantsev, S.L., Levinshtein, M.E., Jackson, A.D., Mohammad, S.N., Harris, G.L., Spencer, M.G., and Shur, M.S., *Properties of Advanced Semiconductor Materials*, pp. 67, New York: Wiley, 2001.
28. Cho, H.-B., Shoji, M., Fujihara, T., Nakayama, T., Suematsu, H., Suzuki, T., and Niihara, K., "Anisotropic Alignment of Non-modified BN Nanosheets in Polysiloxane Matrix under Nano Pulse Width Electricity," *J. Ceram. Soc. Jpn.*, Vol. 118, No. 1373, 2010, pp. 66-69.
29. Wang, Y., Shi, Z., and Yin, J., "Boron Nitride Nanosheets: Large-scale Exfoliation in Methanesulfonic Acid and Their Composites with Polybenzimidazole," *J. Mater. Chem.*, Vol. 21, No. 30, 2011, pp. 11371-11377.
30. Zhi, C., Bando, Y., Tang, C., Kuwahara, H., and Golberg, D., "Large-Scale Fabrication of Boron Nitride Nanosheets and Their Utilization in Polymeric Composites with Improved Thermal and Mechanical Properties," *Adv. Mater.*, Vol. 21, No. 28, 2009, pp. 2889-2893.
31. Lin, Y., Williams, T.V., Xu, T.-B., Cao, W., Elsayed-Ali, H.E., and Connell, J.W., "Aqueous Dispersions of Few-Layered and Monolayered Hexagonal Boron Nitride Nanosheets from Sonication-Assisted Hydrolysis: Critical Role of Water," *J. Phys. Chem. C*, Vol. 115, No. 6, 2011, pp. 2679-2685.
32. Song, X., Gao, J., Nie, Y., Gao, T., Sun, J., Ma, D., Li, Q., Chen, Y., Jin, C., Bachmatiuk, A., Rummeli, M., Ding, F., Zhang, Y., and Liu, Z., "Chemical Vapor Deposition Growth of Large-scale Hexagonal Boron Nitride with Controllable Orientation," *Nano Res.*, 2015, pp. 1-13.

33. Cho, H.-B., Tokoi, Y., Tanaka, S., Suematsu, H., Suzuki, T., Jiang, W., Niihara, K., and Nakayama, T., "Modification of BN Nanosheets and Their Conducting Properties in Nanocomposite Film with Polysiloxane According to the Orientation of BN," *Compos. Sci. Technol.*, Vol. 71, 2011, pp. 1046-1052.
34. Yorifuji, D., and Ando, S., "Enhanced Thermal Diffusivity by Vertical Double Percolation Structures in Polyimide Blend Films Containing Silver Nanoparticles," *Macromol. Chem. Phys.*, Vol. 211, No. 19, 2010, pp. 2118-2114.
35. Fujihara, T., Cho, H.-B., Nakayama, T., Suzuki, T., Jiang, W., Suematsu, H., Kim, H.-D., and Niihara, K., "Field-induced Orientation of Hexagonal Boron Nitride Nanosheets Using Microscopic Mold for Thermal Interface Materials," *J. Am. Ceram. Soc.*, Vol. 95, No. 1, 2012, pp. 369-373.
36. Cho, H.-B., Tokoi, Y., Nakayama, T., Tanaka, S., Jiang, W., Suematsu, H., and Niihara, K., "Facile Orientation of Unmodified BN Nanosheets in Polysiloxane/BN Composite Films Using a High Magnetic Field," *J. Mater. Sci.*, Vol. 46, No. 7, 2011, pp. 2318-2323.